Machine learning based classification of guided wave signals in the context of inter-specimen variabilities

Vivek Nerlikar, Olivier Mesnil, Roberto Miorelli, Oscar D'almeida

Machine Learning Based Classification of Guided Wave Signals in the Context of Inter-specimen Variabilities

Vivek Nerlikar[1(✉)], Olivier Mesnil[1], Roberto Miorelli[1], and Oscar D'Almeida[2]

[1] Université Paris-Saclay, CEA, List, 91129 Palaiseau, France
{vivek.nerlikar,olivier.mesnil,roberto.miorelli}@cea.fr
[2] Safran Tech, Rue des Jeunes Bois, Châteaufort, 78114 Magny-Les-Hameaux, France
oscar.dalmeida@safrangroup.com

Abstract. In the context of Guided Wave-based Structural Health Monitoring (GW-SHM), ultrasonic elastic waves are used to detect damages in structures by comparing the acquired signals with those from a defect-free structure. However, the high sensitivity of GWs to environmental and operational conditions limits the validity of such references. Notably, variabilities between multiple specimens are often significant from the GWs perspective. These variabilities are particularly important in composites and are due to sensor positioning, sensor coupling and material variability. This communication presents a baseline-free approach using physics-enhanced Machine Learning (ML) for enhanced robustness. To ensure the coverage of these variabilities the approach is validated on multiple Carbon-fiber-reinforced polymers (CFRP) panels. The methodology relies on feature extraction from raw GW signals and training classification algorithms (e.g., kernel machines, neural networks). To make the classifier learn inter-specimen variabilities, an experimental database of 45 impacted composite panels is used. Half of them are used to provide pristine data, and the rest to provide damaged data so that the same sample is either in the training or test set, but never in both. Good classification performance is obtained, demonstrating that the classifier has successfully learnt to recognize defect signatures despite the variability linked to the multiple specimens and instrumentations.

Keywords: Guided Waves based SHM · Baseline-free approach · Machine learning · Material and instrumentation variabilities · CFRP

1 Introduction

In Guided Wave-based Structural Health Monitoring (GW-SHM) GWs are used for defect identification in plate-like structures and pipes. Interaction of GWs with a defect modifies the signals and these changes can be identified by comparing the current signal with a reference one, i.e. the signal acquired prior to defect creation.

GWs are not just sensitive to defects but also to material properties, Environmental and Operational Conditions (EOC). The presence of these variabilities makes baseline dependency for defect identification ineffective in many applications [1]. The literature offers a few baseline correction methods which solely focus on temperature effect compensation. Optimal Baseline Selection (OBS) [2], in which residual signal amplitude is minimized until an optimal baseline is selected from the pool of baselines. In a technique called Baseline Signal Stretch (BSS) proposed by A.J. Croxford *et al.* [3], the current signal is stretched until it matches with the baseline. For OBS a big pool of baselines is required which is not practical, whereas BSS alters the frequency content of the signal and is not effective for higher temperatures [1]. There are several methods such as, Dynamic Time Warping (DTW) [4] and OBS+BSS [5], but their main focus is temperature compensation alone. As other EOCs also affect the signals simultaneously, these approaches become ineffective [1].

To overcome the baseline dependency, baseline-free approaches have been proposed. Time reversibility of lamb waves [6], transfer impedance of transducers [7], cross-correlation analysis proposed by Alem *et al.* [8] and other baseline free methods are listed in [1]. The baseline-free techniques utilize mainly signal amplitude, and because EOCs also modify the amplitude of the signal, these techniques become less effective [1].

In recent times, usage of machine learning (ML) and deep learning (DL) is increasing in defect detection and localisation in GW-SHM. Miorelli *et al.* employed post-processed GW-imaging (GWI) to train kernel machines [9], but GWI requires a baseline to obtain the residual state. Schnurr *et al.* [10] worked on detection of temperature affected signals using standard classifiers and features, however the temperature effect was compensated by means of OBS and BSS. Rautela *et al.* [11] showed good classification performance on composite panel using 1D Convolutional Neural Network (CNN). The before-mentioned works depend on baselines and do not present the study of robustness of the developed methodology with respect to multiple identical structures.

ML-based approaches pave the way for baseline-free detection and also can enable the diagnosis of identical structures when trained by considering intra-specimen and inter-specimen variabilities. These are the uncertainties present in single and multiple identical structures, such as sensor coupling, sensor position, and material properties. Therefore, our focus in this study is to address these variabilities by considering multiple CFRP panels and using standard supervised ML approaches augmented by effective feature engineering process.

The following sections of the paper discusses the experimental set up and data-set used. Third section describes the signal preprocessing. Section 4 explains AutoRegression (AR) which is used for extracting features from raw signals. The final two sections present the results obtained by standard ML classifiers and conclusion respectively.

2 Experimental Setup

The experimental set up consists of 45 CFRP plates. Each of the plates is instrumented with 6 piezoelectric sensors distributed over a 150 mm radius circle, one sample instrumented plate is shown in Fig. 1a. In this experiment, delamination type defects are induced by means of impacting each plate with a 16 mm radius steel head and no second impact was allowed. All the 45 coupons are impacted with different energy levels between 3J and 15J at different locations (within circle defined by the sensor network) and an average delamination size ranging from 9.5 mm to 27.5 mm. GW were generated by using a 2 cycle tone burst waveform and at 4 different excitation frequencies namely, 40 kHz, 60 kHz, 80 kHz and 100 kHz. Signal acquisition was carried out by exciting the transducers in round robin fashion, thereby acquiring 30 signals per coupon at a sampling frequency of 5 MHz.

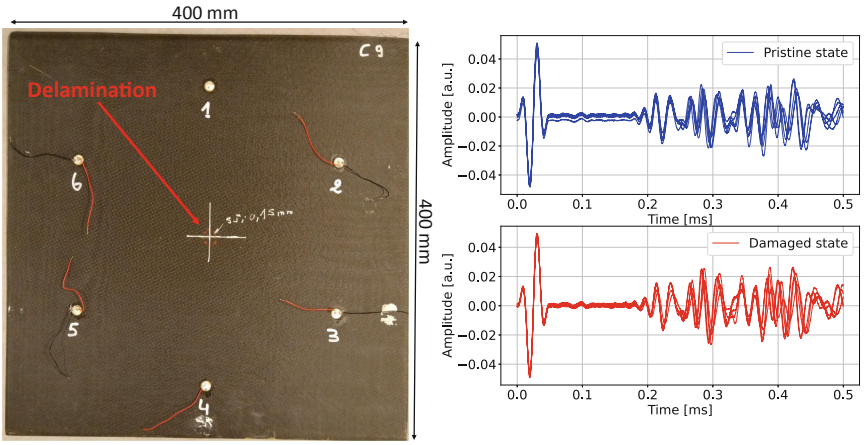

(a) Instrumented plate (b) Sample signals

Fig. 1. (a) Instrumented plate with delamination at the center, (b) 5 sample signals corresponding to path 1–4 of different coupons recorded at 40 kHz

Signal acquisition was first completed on 45 pristine coupons. Later, defect signals were recorded after defect creation. To illustrate the complexity in the signals caused by inter-specimen variability, 5 sample signals of shortened length measured at 40 kHz frequency corresponding to 5 different coupons are shown in Fig. 1. As shown in Fig. 1b, the pristine signals contain variations and do not overlap. This implies the presence of some factors influencing the GW, despite the absence of flaw. These changes can be attributed to the presence of inter-specimen and intra-specimen (variabilities present within one structure) variabilities, which are listed in Table 1. Furthermore, these variabilities not just affect pristine signals but also signals acquired on damaged coupons as illustrated in Fig. 1b. The presence of these variabilities mask the changes due to defect and hence makes defect identification a challenging task.

Table 1. List of intra-specimen and inter-specimen variabilities with level of influence

Variability	Intra-specimen variability	Inter-specimen variability
Measurement noise	Present (more effect)	Present (more effect)
Sensor positioning	Present (less effect)	Present (more effect)
Sensor coupling	Present (less effect)	Present (more effect)
Defect size and shape	Present (more effect)	Present (more effect)
Material properties	Absent	Present

3 Signal Processing and Data Preparation

3.1 Labeling Process: Path Identification

Before using signals for ML processes, it is important to make sure that each of the signals are labeled appropriately. E.g., defect located at the center as shown in Fig. 1a, the adjacent paths (i.e., 1–2, 2–3, 3–4 etc.) might not carry significant defect information. Whereas, direct paths (defect lies between two sensors) (i.e., 1–4, 2–5, 3–6) can carry significant amount of defect information. Such paths need to be labeled as pristine and defect respectively.

The labeling process contains few signal processing steps. Firstly, the signals are filtered using Butterworth bandpass filter of order 7 with the bandpass of 20 kHz and $2 * f_c$ (excitation frequency). Then the filtered signals are windowed using physics of the GWs, i.e., length of the window which is decided based on the Time of Flight (TOF) of the A0 mode and the path. TOF can be calculated based on Eq. (1).

$$TOF_{A0} = \frac{D_t}{C_g^{A_0}(f_c)} \tag{1}$$

where D_t is the distance between transducer pairs and $C_g^{A_0}(f_c)$ is the group velocity of A_0 mode as a function of the f_c. The group velocities are taken from the dispersion diagram.

To identify the paths within defect coupons containing insignificant or no defect information, pristine and defect signals of the same coupons are considered. These signals are processed and are compared based on Root Mean Squared Error (RMSD) as Damage Index (DI), as it can quantify overall changes in the signals [12]. It is calculated based on Eq. (2).

$$RMSD = \sqrt{\frac{\sum_{i=1}^{n}(S_p(i) - S_d(i))^2}{\sum_{i=1}^{n}(S_p(i))^2}} \tag{2}$$

where, S_p and S_d are pristine and damaged signals respectively. $(S_p - S_d)$ is the residual signal, and n is the number of time samples in a signal.

After having defined the processes required, all the paths in defect coupons are compared with the corresponding paths in pristine coupons. RMSD is calculated of each path in a defect coupon. As shown in Fig. 2, direct paths 1–4, 2–5 and 3–6 result in higher DI than non-direct paths. High DIs imply that the corresponding paths carry significant defect information and can be labeled as defect, where as low DIs signify that the paths are carrying insignificant defect information and hence can be labeled as pristine.

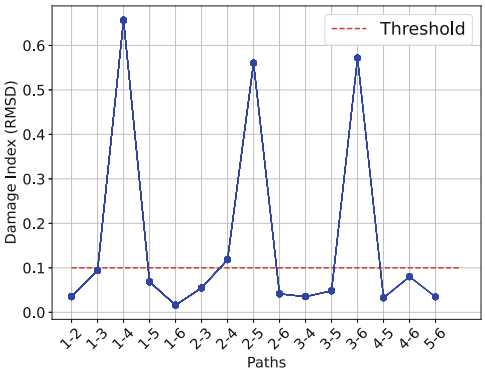

Fig. 2. DI vs paths, for a defect located at the center of the plate

Similar to Fig. 2, plots of DI vs. paths corresponding to coupons with varying defect locations are studied. As a result threshold of 0.1 is chosen, which separates high DI (the result of direct paths) and just lower DI (the result of defect placed slightly away from direct paths) from low DI (the result of defect's presence away from the direct path).

3.2 Disassociating Coupon Connection Between Pristine and Damaged States

As explained in Sect. 2, each one of the coupons has corresponding pristine and damaged states. Before feeding the signals to the ML algorithms, the variance in these two states is further increased by incorporating inter-specimen variabilities, i.e., by dividing 45 coupons into two sets. From 1–22 copouns, only pristine signals are considered. Defect signals are considered from 23–45 coupons only. This step ensures that, none of the pristine or defect signals of same coupon appear neither in training nor in test set; moreover this helps in testing the robustness of ML algorithms. Note, that traditional approaches relying on baseline subtraction such as GWI [13] fail when considering a reference state and a damage state from distinct samples due to the aforementioned inter-specimen variabilities.

4 Defect Detection Methodology

Existing approaches for GW based damage identification involve using raw GW signals to train Convolutional NN (CNN) [11], Principle Component Analysis (PCA) for feature extraction from post processed GW signals and training the extracted features using SVM [9]. In vibration-based SHM, AutoRegression (AR) is used for extracting effective damage features from raw signals under the influence of EOC [14]. Therefore, in this study simple AR modelling technique is used for extracting features. However other modelling techniques such as AR Moving Average (ARMA), AR Integrated Moving Average (ARIMA) methods are available, but AR model has been used in this study for its simplicity interms of implementation.

4.1 Feature Extraction Using Autoregression

After identifying significant and insignificant defect information carrying paths within defect coupons (i.e., path identification), defect signatures masked under the inter-specimen variability are extracted using AR.

AR is a linear combination of preceding values in a sequence [15], a p^{th} order AR model can be represented mathematically as shown in Eq. 3.

$$y(t) = \sum_{i=1}^{p} \Phi_i y(t-i) + \epsilon_t \tag{3}$$

where, y_t is the current observation, $y(t-i)$ is the lag/past value, Φ_i is the AR model parameter and ϵ_t is the white noise term.

Number of past values required are estimated by using suitable information criterion such as, Akaike Information Criteria (AIC) [16]. Computed as,

$$AIC = 2k - 2log(\mathcal{L}) \tag{4}$$

where k is the number of model parameters estimated and $\mathcal{L}$ is the maximum likelihood of the model with k parameters.

A model order of 30 is estimated based on AIC. AR model of order 30 is then fit on all the signals which results in 30 AR features each per signal. Out of 30 features, 3 features showing maximum discrimination between pristine and defect distributions are shown in Fig. 3 in terms of scatter plot matrix, which shows the pairwise dependencies of features. Along the diagonal are the histograms of same pristine and defect AR feature pairs, which show some amount of separation. Kernel Density Estimation (KDE) plots on the off-diagonal, which show the density estimation of distributions of two different AR features pairs. Referring to Fig. 3 it is clear that, histograms and KDE plots show some amount of discrimination. Means that, AR modelling is able to extract some meaningful defect information masked under the effect of variabilities. This discrimination in features can be exploited using ML algorithms. ML-based classification is described in the following section.

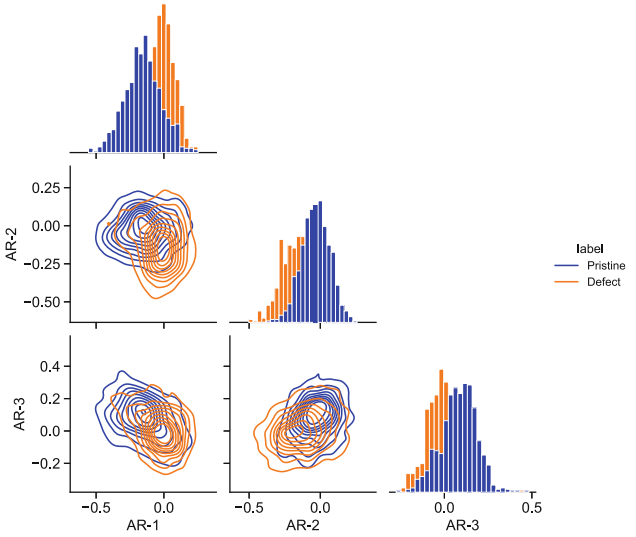

Fig. 3. Scatter plot matrix of first 3 selected features

4.2 Classification

To perform ML-based classification, four different families of classifiers have been considered. The consideration of these four families is to study the effectiveness of each of them in learning the encoding generated by AR. These four classifiers are briefly explained below.

Naive Bayes (NB) classifier. It is based on Bayes theorem, which states that the probability of occurrence of an event could be related to the prior information of the event. A sample A is classified as P class B if and only if $p(B = P|A) \geq p(B = N|A)$ [17]

Support Vector Machines (SVM). SVM handles a classification task by building a decision boundary (known as hard margin) and tries to maximize the width (soft margin) between two classes. Training samples which are closest to the decision boundary are called as the support vectors [18]. The decision boundaries can be drawn using linear or non-linear kernels depending on the complexity of the training data.

Random Forest (RF). It is an ensemble learning method which contains more than one decision trees. Each of the tree gets independent and randomly sampled samples with same distribution. The final prediction of RF is the combined votes of each of the trees [19].

Deep Neural Network (DNN). It consists of multiple hidden layers along with an input and output layer. The hidden layers contain the information about the inputs in terms of weights. These weights are optimized by minimizing the cost function based on the back propagation algorithm [20].

5 Experimental Validation Results

5.1 Data Requirement Study

The goal here is to choose the best ML model given an algorithm. To find the best model, a trade-off between training samples and AR features is required. For this 5 different train and validation sets with increasing training samples, i.e., (88, 221, 443, 664, 886) and validation samples, i.e., (22, 56, 111, 167, 222) are considered, and AR features from 4 to 28 in step of 6, i.e., (4, 10, 16, 22, 28) are considered. For SVM, 'rbf' kernel is used with regularization parameter C and kernel coefficient γ chosen from $10^c, c \in (-1, 7)$ and $10^\gamma, \gamma \in (1, -7)$ respectively. On each train set and AR features, best ML model from the range of hyper-parameters is selected using Gridsearch Cross Validation (CV) technique.

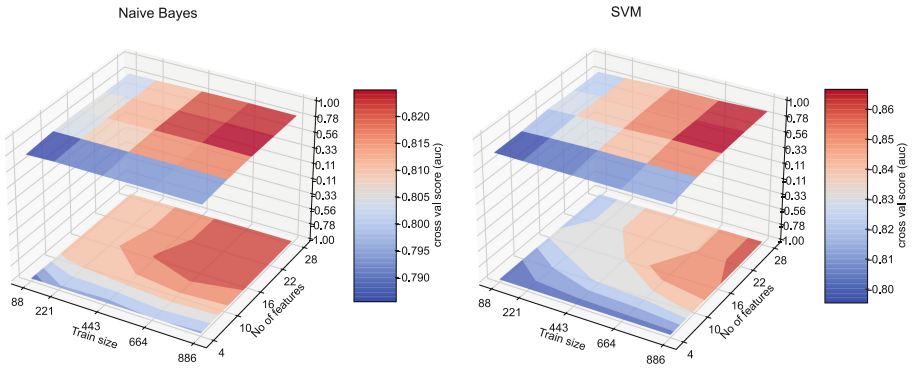

(a) Naive Bayes (b) SVM

Fig. 4. Learning curves as a function of training samples and AR features.

Figure 4 shows the learning curve of NB and SVM classifier on train size and AR features. From Fig. 4a and Fig. 4b it can be observed that, CV score converges at 600 train samples and 16 AR features for NB, and at 800 train samples and 20 AR features for SVM respectively. Based on the convergence study of one simple and a sophisticated classifier, training samples of 886 with 20 AR features have been picked to train all the classifiers listed in the previous section and have been tested on the held out test-set.

5.2 Performance Comparison

Figure 5 present the Receiver Operating Characteristics (ROC) Curve on the test-set. It contains ROC curves of NB, SVM, Random Forest and DNN along with the estimated Area Under the Curve (AUC). It can be observed that the AUC of NB is 0.89 and for rest of the classifiers it is between 0.91 and 0.92. Such value shows that the classifiers have successfully learned the features related to the damage in the signals and most signals are well-classified.

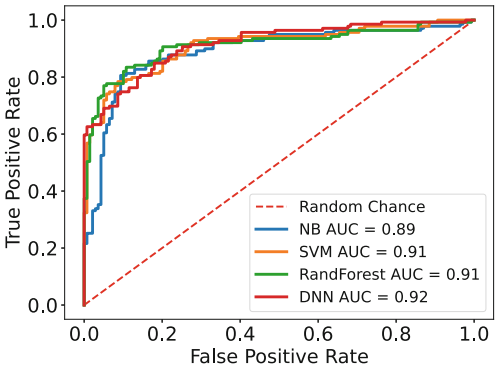

Fig. 5. ROC curves of all classifiers comparing their performances.

6 Conclusion and Perspective

In this work a baseline-free damage detection approach based on ML applied to CFRP measurement data is presented. The classifiers were trained and the performance was assessed on measurement data with inter-specimen variability. To ensure learning the inter-specimen variabilities, distinct samples have been used to learn the pristine state and the damage states. AUC of the order 91% was obtained for all classifiers, implying that, all the classifiers except for NB are equally good in learning to distinguish pristine from defect state in the presence of variabilities. Among SVM, Random Forest and DNN, SVM takes less time for training and testing the model. Also in terms of model complexity, SVM requires fewer hyper-parameters; therefore SVM is a better choice on this data set than others. The high AUC value means that the classification is correct for most signals but there is still room for improvement.

References

1. Gorgin, R., Luo, Y., Wu, Z.: Environmental and operational conditions effects on lamb wave based structural health monitoring systems: a review. Ultrasonics **105**, 106114 (2020)
2. Lu, Y., Michaels, J.E.: A methodology for structural health monitoring with diffuse ultrasonic waves in the presence of temperature variations. Ultrasonics **43**(9), 717–731 (2005)
3. Croxford, A.J., Wilcox, P.D., Konstantinidis, G., Drinkwater, B.W.: Strategies for overcoming the effect of temperature on guided wave structural health monitoring. In: Kundu, T. (ed.) Health Monitoring of Structural and Biological Systems 2007, vol. 6532, pp. 590–599. International Society for Optics and Photonics, SPIE (2007)
4. Douglass, A.C.S., Harley, J.B.: Dynamic time warping temperature compensation for guided wave structural health monitoring. IEEE Trans. Ultrason. Ferroelectr. Freq. Control **65**(5), 851–861 (2018)

5. Croxford, A.J., Moll, J., Wilcox, P.D., Michaels, J.E.: Efficient temperature compensation strategies for guided wave structural health monitoring. Ultrasonics **50**(4–5), 517–528 (2010)
6. Ing, R.K., Fink, M.: Self-focusing and time recompression of lamb waves using a time reversal mirror. Ultrasonics **36**(1–5), 179–186 (1998)
7. Park, S., Lee, C., Sohn, H.: Reference-free crack detection using transfer impedances. J. Sound Vib. **329**(12), 2337–2348 (2010)
8. Alem, B., Abedian, A., Nasrollahi-Nasab, K.: Reference-free damage identification in plate-like structures using lamb-wave propagation with embedded piezoelectric sensors. J. Aerosp. Eng. **29**(6), 04016062 (2016)
9. Miorelli, R., Kulakovskyi, A., Chapuis, B., D'Almeida, O., Mesnil, O.: Supervised learning strategy for classification and regression tasks applied to aeronautical structural health monitoring problems. Ultrasonics **113**, 106372 (2021)
10. Schnur, C., et al.: Towards interpretable machine learning for automated damage detection based on ultrasonic guided waves. Sensors **22**(1), 406 (2022)
11. Rautela, M., Senthilnath, J., Moll, J., Gopalakrishnan, S.: Combined two-level damage identification strategy using ultrasonic guided waves and physical knowledge assisted machine learning. Ultrasonics **115**, 106451 (2021)
12. Xu, B., Giurgiutiu, V.: Single mode tuning effects on lamb wave time reversal with piezoelectric wafer active sensors for structural health monitoring. J. Nondestr. Eval. **26**(2–4), 123–134 (2007)
13. Hall, J.S., Michaels, J.E.: Multipath ultrasonic guided wave imaging in complex structures. Struct. Health Monit. **14**(4), 345–358 (2015)
14. Cheng, J., Yu, D., Yang, Y.: A fault diagnosis approach for gears based on IMF AR model and SVM. EURASIP J. Adv. Signal Process. **2008**(1) (2008)
15. Montgomery, D.C., Jennings, C.L., Kulahci, M.: Introduction to Time Series Analysis and Forecasting. Wiley Series in Probability and Statistics, 2nd edn. (2015)
16. Akaike, H.: A new look at the statistical model identification. IEEE Trans. Autom. Control **19**(6), 716–723 (1974)
17. Zhang, H.: The optimality of Naïve Bayes. In: FLAIRS2004 Conference (2004)
18. Boser, B.E., Guyon, I.M., Vapnik, V.N.: A training algorithm for optimal margin classifiers. In: Proceedings of the Fifth Annual Workshop on Computational Learning Theory - COLT 1992. ACM Press (1992)
19. Breiman, L.: Random forests. Mach. Learn. **45**(1), 5–32 (2001)
20. Chollet, F.: Deep Learning with Python. Manning Publications (2017)